The Objective Prediction of Clouds and Precipitation Using Vertically Integrated Moisture and Adiabatic Vertical Motions

RUSSELL J. YOUNKIN, JERROLD A. LARUE
National Meteorological Center, U. S. Weather Bureau, Suitland, Md.
AND FREDERICK SANDERS
Massachusetts Institute of Technology, Cambridge, Mass.

(Manuscript received 27 January 1964, in revised form 9 November 1964)

ABSTRACT

This article describes and illustrates an objective technique of forecasting clouds, precipitation and precipitation amounts. The system is tailored to fit the specific operation of the National Meteorological Center in the use of data routinely available. It attempts to eliminate or to alleviate a number of difficulties which have plagued other objective techniques.

The method follows rather closely the earlier work of Frederick Sanders, but departs importantly in the method of obtaining vertical motion and in the form and manipulation of the moisture parameter. The vertical motion is computed from objective 1000-mb and 500-mb prognoses through an adiabatic approach. Saturation thickness is used as the moisture parameter in a manner which eliminates the need for reference to specific and relative humidities.

Two forecasts are illustrated in detail. The first example employs a form which obtains directly a vertical motion field, while the second by-passes this step.

1. Introduction

The need for objective assistance in cloud and precipitation forecasting has become apparent during the past few years in that the additional information provided by numerical weather prognostic (NWP) charts has failed to improve appreciably the forecasts of these elements. This additional NWP material has led to the development of new models to be used as a basis for subjective cloud and weather prediction and has added to the sophistication of older models. The increasing accuracy of the NWP predictions of upper air circulation has resulted in these models becoming more and more dependent upon upper levels.

These developments encouraged the centralization of cloud and weather forecasting, and the Analysis and Forecast Division of the U. S. Weather Bureau commenced issuing forecasts of the instantaneous occurrence of cloud and weather for the United States area in February of 1960. Almost four years verification of these forecasts reveals only one significant trend in skill, and this was incurred by specialization of personnel making the forecasts. While comparative verification of the forecasts with those issued by other offices of the U. S. Weather Bureau are not completely satisfactory due to differences in the formats, those that have been made, indicate only small differences in skills.

A cloud and weather forecasting experiment was conducted during 1964 by the Analysis and Forecast Division. It involved the use of observed contour data (perfect progs) to specify contemporary cloud and precipitation conditions. That is, forecasters were instructed to supply the cloud and precipitation patterns associated with contour analyses of observed surface and upper air data. Ten cases were chosen such that five of the originally transmitted operational forecasts had scored well and five poorly. Each case was forecast by ten forecasters of varied experience. In general, the skill scores were disappointingly low. Scores for the five poor cases averaged higher than the original forecasts, but those for the good forecasts averaged lower. The one encouraging fact to emerge was that the forecaster who specialized operationally in cloud and weather forecasting averaged very significantly higher.

It appears the subjective forecasts of cloud and precipitation phenomena have advanced about as far as is possible even with the aid of related objectively forecast parameters. Further improvement must come from objective methods which can handle the parameters in a systematic manner. Due to the number and nature of the processes involved, it is probable, at least when dealing with large areas, that an operationally successful objective system must be dependent upon numerical assistance.

2. Resume of objective cloud and precipitation forecasting techniques

A number of objective cloud and precipitation forecasting methods has been developed during the past

ten years, for example, Thomson and Collins (1953), Spar (1953), Kuhn (1953), Collins and Kuhn (1954), Smagorinski and Collins (1955), Swayne (1956), Estoque (1958), Sanders (1958), Smeybe (1958), George *et al.* (1960), and Vederman (1961). These investigators employed the physical approach which necessitates an evaluation of the moisture and vertical motion fields. A measure of the moisture content of the air is obtained from upper air observations. Then the moisture field is usually transported by the wind at some level or levels. An attempt is made to approximate the effect of vertical motion on the degree of saturation which is then related to cloud and weather occurrence through statistical or theoretical studies.

It is assumed in cloud and weather forecasting that, when the water vapor pressure of an air parcel equals the saturation vapor pressure, condensation will occur. It is necessary, therefore, that a parameter or parameters be used which will provide a measure of the ratio or difference between these two vapor pressures. The relative humidity, for example, satisfies this condition. In general, then, the forecast problem for the occurrence of clouds and precipitation becomes one of forecasting the relative humidity, or parameters from which the relative humidity may be derived. If precipitation amounts are also a goal of the forecasts then an additional parameter may be required to provide a measure of the quantity of moisture.

Numerical techniques have been limited in the past to using data reported at mandatory isobaric levels. Since the vertical profile of moisture is highly variable these levels often misrepresent the moisture content. This has been a great disadvantage to the numerical approach. Recently the National Meteorological Center incorporated the entire radiosonde observation into its automatic data processing program. This has made possible machine integration of the moisture content of the air and the evaluation of a mean relative humidity. Numerical techniques which take advantage of this opportunity for use of an integrated moisture parameter may prove more successful than past efforts.

Some hand operated systems use a vertically integrated moisture parameter. These usually depend upon the precipitable water data available on the National Weather Facsimile Circuit. While the precipitable water has been utilized directly by some techniques, others have compared it with the mean temperature of the column in order to change it to a measure of the degree of saturation. If used directly, the precipitable water is later related to the mean forecast temperature so as to produce the forecast degree of saturation. If changed to a degree of saturation form prior to forecast displacement, it may still be necessary that it be compared to the forecast temperature should a forecast of absolute humidity or precipitation amount be desired.

In our experience, at the Analysis and Forecast Division, difficulties have arisen in the use of routinely available vertical motions for cloud and precipitation forecasting. These motions often appear to be too small. The result has often been that the effect of horizontal moisture advection predominates unduly over modification due to vertical motion, so that in time the forecast systems become synoptically inconsistent with the predicted pressure patterns. Use of somewhat larger vertical motions obtained by graphical means, also, is unsatisfactory, probably because of the crudeness of assumptions which must be made in the interest of practicality. An unquestioned advantage of numerical computation over graphical methods, finally, is the shortness of the time steps which may be taken in the former approach.

3. Theoretical development

The "precipitable water," as the term is now used in NMC, is the liquid depth of the mass of water vapor in a column of unit horizontal cross section extending from the surface of the earth to the 500-mb level. For the purpose of this discussion we shall consider W, the mass of water vapor in such a column extending through the entire depth of the atmosphere. Thus,

$$W \equiv \frac{1}{g}\int_0^{\pi} q\,dp, \tag{1}$$

where q is the specific humidity and π is the pressure at the surface of the earth. For convenience we shall refer to W as the precipitable water.

Because of the especially great importance of dealing adequately with the conditions at the lower boundary in forecasting the water vapor, and because of the considerable difficulties raised by mountains in a formulation in the (x,y,p,t)-coordinate system, we shall use $\sigma \equiv p/\pi$ (Phillips, 1957) as a vertical coordinate. In this system, Eq. (1) becomes

$$W \equiv \frac{\pi}{g}\int_0^{1} q\,d\sigma. \tag{2}$$

On the assumption that no evaporation or condensation occurs, the specific humidity is a conservative property. Let us think of such a quantity as a "virtual" specific humidity, q', and regard W' as a "virtual" precipitable water, following the convention of the Staff Members of Tokyo University (1955).

Now in the σ-system the conservation of q' is expressed by

$$\frac{dq'}{dt} = \frac{\partial q'}{\partial t} + \mathbf{V}\cdot\nabla q + \dot{\sigma}\frac{\partial q}{\partial \sigma} \quad 0 \tag{3}$$

while the principle of conservation of mass is given by

$$\nabla\cdot\pi\mathbf{V} + \pi\frac{\partial \dot{\sigma}}{\partial \sigma} + \frac{\partial \pi}{\partial t} = 0, \tag{4}$$

where $\dot{\sigma} \equiv d\sigma/dt$. Eqs. (3) and (4) may be combined to yield the following prediction equation for q' on a σ-surface:

$$\frac{\partial q'}{\partial t} = -\mathbf{V}\cdot\nabla q - q\nabla\cdot\mathbf{V} - \frac{\partial q\dot{\sigma}}{\partial \sigma} - \frac{q}{\pi}\left(\frac{\partial \pi}{\partial t} + \mathbf{V}\cdot\nabla\pi\right) \quad (5)$$

Partial differentiation of (2) with respect to time yields

$$\frac{\partial W'}{\partial t} = \frac{\pi}{g}\int_0^1 \frac{\partial q'}{\partial t} d\sigma + \frac{W}{\pi}\frac{\partial \pi}{\partial t}. \quad (6)$$

Since $\dot{\sigma}$ vanishes at the top and bottom of the atmosphere (at $\sigma=0$) and ($\sigma=1$), substitution from (5) in (6) followed by integration then gives the prediction equation for virtual precipitable water:

$$\frac{\partial W'}{\partial t} = \frac{\pi}{g}\int_0^1 (-\mathbf{V}\cdot\nabla q)d\sigma + \frac{\pi}{g}\int_0^1 (-q\nabla\cdot\mathbf{V})d\sigma + \frac{1}{g}\int_0^1 (-q\mathbf{V}\cdot\nabla\pi)d\sigma. \quad (7)$$

Since the right side of (7) can be expressed as

$$\frac{1}{g}\int_0^1 \nabla\cdot\pi q\mathbf{V} d\sigma$$

it is apparent that integration of (7) over the entire earth confirms the conservation of total virtual precipitable water in the atmosphere. This finding is physically consistent with the assumption of neither sources nor sinks for the virtual specific humidity.

The heart of this forecast method resides in the proposition that the integrals in (7) can be evaluated with sufficient accuracy by modeling the vertical variations of q, $\mathbf{V}$, and $\nabla\cdot\mathbf{V}$. This approach is admittedly heuristic and somewhat inconsistent and is based primarily on an appeal to the observational evidence. Analogous assumptions, moreover, have proved useful in circulation prognosis. In the light of these disclaimers we then assume

$$q'(x,y,\sigma,t) = \alpha(\sigma)\frac{gW'(x,y,t)}{\pi(x,y,t)}, \quad (8)$$

where $\alpha(\sigma)$ is a modeling parameter to be obtained from climatological moisture soundings

$$\mathbf{V}(x,y,\sigma,t) = [1-\beta(\sigma)]\mathbf{V}_1(x,y,t) + \beta(\sigma)\bar{\mathbf{V}}(x,y,t), \quad (9)$$

where $\beta(\sigma)$ is another modeling parameter to be determined by climatological wind data

$$\nabla\cdot\mathbf{V}(x,y,\sigma,t) = -\frac{1}{\pi}\frac{\partial \pi}{\partial t}(x,y,t) - \frac{1}{\pi}\bar{\mathbf{V}}\cdot\nabla\pi(x,y,t) - [1-\beta(\sigma)][\nabla\cdot\bar{\mathbf{V}} - \nabla\cdot\mathbf{V}_1]. \quad (10)$$

Here $(\overline{\quad}) \equiv \int_0^1 (\quad) d\sigma$, an average with respect to pressure through the entire depth of the atmosphere, and the subscript one denotes the value of the quantity at the level where $\sigma=1$, i.e., at the surface of the earth. From (1) we find that $\bar{\alpha}=1$ while from (9) we see that $\bar{\beta}=1$ and that $\beta_1=0$. The rather complex form of (10) stems from the thought that the integrated divergence ought to satisfy the surface pressure tendency equation

$$\frac{\partial \pi}{\partial t} = -\int_0^1 \nabla\cdot\pi\mathbf{V} d\sigma. \quad (11)$$

In evaluating the second term on the right side of (7) it will be useful to relate $\nabla\cdot\mathbf{V}_1$ to $\dot{\sigma}_m$. (Here the subscript m refers to the σ-surface where $\mathbf{V}=\bar{\mathbf{V}}$). The required relationship is obtained by integration of (4):

$$\pi\dot{\sigma}_m = -\int_0^{\sigma_m} \nabla\cdot\pi\mathbf{V} d\sigma - \sigma_m\frac{\partial \pi}{\partial t}. \quad (12)$$

Substitution of (9) and (10) in this equation leads to

$$\nabla\cdot\mathbf{V}_1 = -\pi^{-1}\frac{\partial \pi}{\partial t} - \pi^{-1}\mathbf{V}_1\cdot\nabla\pi - \dot{\sigma}_m\left[\int_0^{\sigma_m}(1-\beta)d\sigma\right]^{-1}. \quad (13)$$

To evaluate the integrals in (7) we now substitute in this equation from (8), (9), (10) and (13). The result is

$$\frac{\partial W'}{\partial t} = -(K_1\mathbf{V}_1 + K_2\bar{\mathbf{V}})\cdot\nabla W - WK_3\dot{\sigma}_m + \frac{W}{\pi}\frac{\partial \pi}{\partial t}, \quad (14)$$

where

$$K_1 \equiv 1-\overline{\alpha\beta},$$

$$K_2 \equiv \overline{\alpha\beta},$$

$$K_3 \equiv [1-\overline{\alpha\beta}]\left[\int_0^{\sigma_m}(\beta-1)d\sigma\right]^{-1}.$$

If $\omega = dp/dt$ is to be used as a measure of vertical motion instead of $\dot{\sigma}$, the following relationship between the two may be employed:

$$\dot{\sigma}_m = \frac{1}{\pi}\left[\omega_m - \sigma_m\left(\frac{\partial \pi}{\partial t} + \bar{\mathbf{V}}\cdot\nabla\pi\right)\right]. \quad (15)$$

The prediction equation for virtual precipitable water then becomes

$$\frac{\partial W'}{\partial t} = -(K_1\mathbf{V}_1 + K_2\bar{\mathbf{V}})\cdot\nabla W' - \frac{WK_3}{\pi}\omega_m + \frac{W\sigma_m K_3}{\pi}\bar{\mathbf{V}}\cdot\nabla\pi + \frac{W}{\pi}(1+\sigma_m K_3)\frac{\partial \pi}{\partial t}. \quad (16)$$

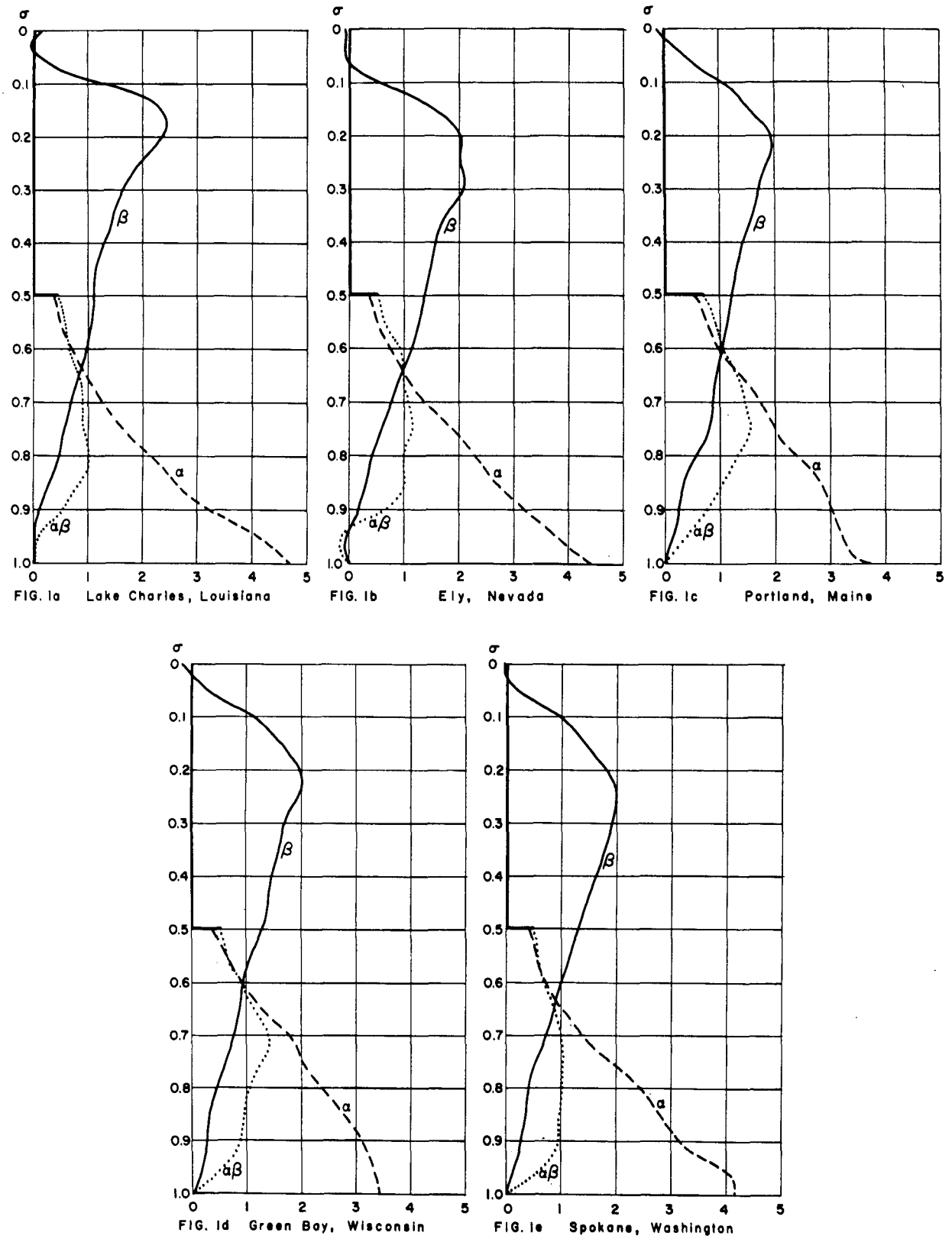

FIG. 1. Vertical profiles of α, β and $\alpha\beta$ obtained from April 1962 mean sounding data.

In (14) the effect of sloping terrain is included in the $\dot{\sigma}$ term; in (16) it appears explicitly in the $\bar{\mathbf{V}}\cdot\nabla\pi$ term. In either equation the term containing $\partial\pi/\partial t$ is probably negligible in comparison with others. It is not entirely clear under what circumstances (14) conserves the total virtual precipitable water in the entire atmosphere. One way to achieve conservation would be to use a nondivergent wind in the advection terms and to make all the coefficients constant. Unfortunately, since the winds are taken on a σ-surface and since W is highly variable neither of these assumptions seems very palatable. The point should be examined further.

4. Evaluation of the coefficients

For practical purposes we should consult the observational evidence for determination of optimum values of the constants K_1, K_2, and K_3. A start in this direction was made by obtaining values from monthly mean sounding data for Lake Charles (72240), Ely(72486), Portland (72606), Green Bay (72645), and Spokane (72785) from Climatological Data for April 1962. It was assumed that q dropped discontinuously to zero at $\sigma=0.5$, since few moisture data were available above this level. Where humidity data were missing below this level, a relative humidity of 30 per cent was assumed. Values of β were taken from the total wind speed unless the direction varied appreciably, when only the westerly component was used. Profiles of α, β, and $\alpha\beta$ for each of these stations are shown in Fig. 1a–e. Values of π, V_1 or (u_1), $\bar{V}$ (or $\bar{u}$), $\bar{q}$, K_1, K_2, $K_3\sigma_m$, σ_*, and p_*, are given in Table 1. The last two of the above quantities are the σ-level and the pressure level at which $V=K_1V_1+K_2\bar{V}$ (or $\bar{u}=K_1u_1+K_2\bar{u}$), i.e., the effective "moisture steering level." If it had been assumed that q varied linearly from its value at $\sigma=0.5$ to zero at $\sigma=0$, K_2 would have been increased (and K_1 decreased) by about 0.10 and the effective moisture steering level would have been elevated about 30 mb. It is likely that the profiles of α suffer from bias in the published mean humidity data. The amount of this bias is undetermined but its elimination would probably tend to bring the effective moisture steering level somewhat closer to the ground. Finally, the speed of the resultant wind near the ground probably underestimates the low-level moisture advection. Correction of this bias would also tend to lower the effective moisture steering level. From (16) and the data in Table 1 it can be shown that the time-integral of ω_m required to effect a two-fold increase in W' ranges from 186 mb at Lake Charles to 260 mb at Portland.

The values in Table 1 are consistent with those found by Sanders (1963) in a survey of mean soundings for October 1960 in a formulation of the problem in the (x,y,p,t)-system, and with climatological results reported recently by Reitan (1963). The results in Table 1, however, are more variable from station to station and show rather large values of K_3. A comparison among stations shows that a high concentration of moisture at low levels (e.g., at Lake Charles) tends to make K_1 and K_3 particularly large. This result is physically consistent with the modeling assumptions. The strong dependence of p_* upon π illustrates the desirability of working in the σ-system. Clearly more monthly mean and individual daily data must be examined before optimum values of the coefficients can be established with confidence.

5. An operational model

At present it is not possible to fashion an operational prediction model directly from the theory presented above, because initial and predicted winds and vertical motions refer to constant-pressure surfaces. Moreover, available predicted temperatures are mean values (i.e., thicknesses) between fixed constant-pressure surfaces. We shall now propose an operational model which is at least related to the foregoing theory and which uses currently available objective parameters—observed precipitable water, 500-mb and 1000-mb data, and numerical prognoses for 500 mb and 1000 mb (Reed, 1963).

First, it will be necessary to write (16) as

$$\frac{\partial W'}{\partial t}=-\mathbf{V}_*\cdot\nabla W-\frac{WK_3}{1000\text{ mb}}\omega_m+\frac{W\sigma_mK_3}{1000\text{ mb}}\mathbf{V}_5\cdot\nabla\pi. \quad (17)$$

Here $\mathbf{V}_*\equiv K_1\mathbf{V}_0+K_2\mathbf{V}_5$, where $\mathbf{V}_0$ and $\mathbf{V}_5$ are the 1000-mb and 500-mb winds, respectively. The subscript m refers to the level where the wind is equal to the mean wind in the (x,y,p,t) system. The term in (16) containing $\partial\pi/\partial t$ has been dropped. Next we shall express the observed virtual precipitable water in terms of h_s, the "saturation thickness," as suggested by Swayne (1956).

TABLE 1. Moisture prediction parameters for selected mean sounding in April 1962.

Station	π (mb)	V_1 or u_1 (kts)	$\bar{V}$ or $\bar{u}$ (kts)	$\bar{q}$ (g kg^{-1})	K_1	K_2	K_3	σ_m	σ_*	p_*
Lake Charles (72240)	1017	−2	24	2.04	0.72	0.28	4.0	0.58	0.86	878
Ely (72486)	810	2	19	0.79	0.63	0.37	3.0	0.64	0.84	680
Portland (72606)	1012	3	28	1.02	0.49	0.51	2.7	0.63	0.80	812
Green Bay (72645)	991	3	21	0.94	0.54	0.46	2.7	0.58	0.80	790
Spokane (72785)	932	0	24	1.00	0.60	0.40	2.9	0.60	0.81	754

This is the thickness of the layer from 100 mb to 500 mb which has a uniform relative humidity of 70 per cent and a moist-adiabatic lapse rate and which contains a mass of water vapor equal to the observed precipitable water. The use of the 70 per cent value to connote saturation is justified by the low bias in relative humidity values reported by radiosonde and by the abundant observational evidence that overcast clouds and precipitation are likely even when parts of the air-column are unsaturated. Thus,

$$h_s = h_s(W); \quad \pi = 1000 \text{ mb}. \tag{18}$$

The relationship between h_s and W is given in Table 2, where the latter quantity is given in liquid depth to conform with current practice. The degree of saturation will ultimately be expressed by the difference between h_5, the observed thickness from 1000 mb to 500 mb, and the saturation thickness. Thus the "saturation deficit," h_d, is given by

$$h_d \equiv h_5 - h_s. \tag{19}$$

This relationship will not give a good estimate of the degree of saturation at high elevations where π is far from 1000 mb. An adjusted value of precipitable water, W_a, which is not inconsistent with the adjusted temperature used in obtaining h_5, can be obtained by adopting a reasonable profile of $\alpha(p)$ for the entire air column from 1000 mb to the top of the atmosphere. A fictitious amount of water vapor for the part of the column from π to 1000 mb is added to the observed amount. This added amount is equal to the observed amount multiplied by the ratio between the integral of α between 1000 mb and π to the integral of α between π and the top of the atmosphere. This addition can be effected by setting

$$W_a = W\left(1000 \text{ mb} \Big/ \int_0^{\pi} \alpha dp\right).$$

The profiles in Fig. 1 and the data in Table 2 then suggest appropriate corrections to unadjusted saturation thickness (h_{su}, π not at 1000 mb) values to obtain uniformly consistent values of h_s. These corrections are given in Table 3. The unadjusted saturation deficit (h_{du}) corresponding to the unadjusted saturation thickness (h_{su}) is given by

$$h_{du} = h_5 - h_{su}. \tag{20}$$

Now in view of (18), it follows that

$$\frac{\partial W'}{\partial t} = \frac{dW}{dh_s}\frac{\partial h_s}{\partial t} \tag{21}$$

so that (17) can be written in the form

$$\frac{\partial h_s}{\partial t} = -\mathbf{V}_* \cdot \nabla h_s - K_4 \omega_m + \mathbf{V}_5 \cdot \nabla P'(\pi), \tag{22}$$

where,

$$K_4 \equiv \frac{K_3}{1000 \text{ mb}}\left(\frac{W dh_s}{dW}\right)$$

and

$$P'(\pi) \equiv \frac{\pi K_3 \sigma_m}{1000 \text{ mb}}\left(\frac{W dh_s}{dW}\right).$$

A constant value of $W dh_s/dW$ must be chosen for the evaluation of K_4 and P'. From the data in Table 2 it can be seen that this quantity varies by a factor of about three and that a reasonable average value is 300 meters. If, now, we select $K_3 = 2.6$ and $\sigma_m = 0.6$, then $K_4 = 0.8m$ mb^{-1} and $P'(\pi) = 468(\pi/1000 \text{ mb})\ m$.

Eq. (22) provides a forecast of the absolute humidity. To predict clouds and precipitation we must find a prediction equation for the saturation deficit. The

TABLE 2. Precipitable water (W) and corresponding saturation thickness (h_s) for 70 per cent humidity from 1000 mb to 500 mb.

W inches	h_s gpm	W inches	h_s gpm	W inches	h_s gpm
0.03	4644	0.38	5283	0.96	5582
0.04	4705	0.39	5291	0.98	5589
0.05	4756	0.40	5299	1.00	5596
0.06	4799	0.41	5307	1.05	5612
0.07	4835	0.42	5314	1.10	5628
0.08	4866	0.43	5321	1.15	5643
0.09	4892	0.44	5328	1.20	5658
0.10	4916	0.45	5335	1.25	5672
0.11	4938	0.46	5342	1.30	5686
0.12	4960	0.47	5349	1.35	5699
0.13	4981	0.48	5356	1.40	5712
0.14	5000	0.49	5363	1.45	5724
0.15	5019	0.50	5369	1.50	5735
0.16	5036	0.52	5381	1.55	5746
0.17	5052	0.54	5393	1.60	5757
0.18	5067	0.56	5404	1.65	5768
0.19	5082	0.58	5415	1.70	5779
0.20	5098	0.60	5426	1.75	5789
0.21	5112	0.62	5437	1.80	5799
0.22	5126	0.64	5446	1.85	5809
0.23	5139	0.66	5456	1.90	5819
0.24	5151	0.68	5466	1.95	5828
0.25	5163	0.70	5476	2.00	5837
0.26	5174	0.72	5485	2.10	5854
0.27	5184	0.74	5494	2.20	5870
0.28	5194	0.76	5503	2.30	5886
0.29	5203	0.78	5512	2.40	5902
0.30	5213	0.80	5521	2.50	5917
0.31	5223	0.82	5529	2.60	5932
0.32	5232	0.84	5537	2.70	5947
0.33	5241	0.86	5545	2.80	5961
0.34	5250	0.88	5553	2.90	5974
0.35	5259	0.90	5561	3.00	5987
0.36	5267	0.92	5568		
0.37	5275	0.94	5575		

TABLE 3. Adjustment in saturation thickness due to station pressure.

π (mb)	1000	950	900	850	800	750	700
$[h_s - h_{su}]$ (dm)	0	8	16	24	32	41	52

thermodynamic-energy equation for adiabatic processes may be written in the (x,y,p,t)-system

$$\frac{\partial}{\partial t}\left(\frac{\partial z}{\partial p}\right)=-\mathbf{V}\cdot\nabla\left(\frac{\partial z}{\partial p}\right)-\left(\frac{1}{\theta}\frac{\partial z}{\partial p}\frac{\partial \theta}{\partial p}\right)\omega. \tag{23}$$

Integration of this equation from 1000 mb to 500 mb, on the assumption that the direction of the vertical wind shear does not change with height, yields

$$\frac{\partial h_5}{\partial t}=-\mathbf{V}_*\cdot\nabla h_5+\int_{500\text{ mb}}^{1000\text{ mb}}\left(\frac{1}{\theta}\frac{\partial z}{\partial p}\frac{\partial \theta}{\partial p}\right)\omega dp. \tag{24}$$

To evaluate the integral in (24) we start by expressing ω in terms of ω_0 and ω_m (the values at 1000 mb and at the "mean level"). This can be accomplished by modeling the vertical variation of the divergence:

$$\nabla\cdot\mathbf{V}(x,y,p,t)$$
$$=-\frac{\omega_0(x,y,t)}{1000\text{ mb}}-[1-\beta(p)][\nabla\cdot\overline{\mathbf{V}}-\nabla\cdot\mathbf{V}_0](x,y,t). \tag{25}$$

This expression is similar to Eq. (10) in the σ-system. Integration of the mass continuity equation

$$\frac{\partial\omega}{\partial p}=-\nabla\cdot\mathbf{V}$$

then gives the following formula for ω:

$$\omega(x,y,p,t)=\left\{\frac{p}{1000\text{ mb}}\left[1-\frac{\int_0^p(1-\beta)dp}{\int_0^{p_m}(1-\beta)dp}\right]\right\}\omega_0$$
$$+\left[\frac{\int_0^p(1-\beta)dp}{\int_0^{p_m}(1-\beta)dp}\right]\omega_m. \tag{26}$$

Upon substitution from (26) in Eq. (24) we have

$$\frac{\partial h_5}{\partial t}=-\mathbf{V}_*\cdot\nabla h_5+K_5\omega_0+K_6\omega_m, \tag{27}$$

where

$$K_5\equiv\int_{500\text{ mb}}^{1000\text{ mb}}\frac{1}{\theta}\frac{\partial z}{\partial p}\frac{\partial\theta}{\partial p}\left\{\frac{p}{1000\text{ mb}}\left[1-\frac{\int_0^p(1-\beta)dp}{\int_0^{p_m}(1-\beta)dp}\right]\right\}dp$$

and

$$K_6\equiv\int_{500\text{ mb}}^{1000\text{ mb}}\frac{1}{\theta}\frac{\partial z}{\partial p}\frac{\partial\theta}{\partial p}\left[\frac{\int_0^p(1-\beta)dp}{\int_0^{p_m}(1-\beta)dp}\right]dp.$$

Use of winter climatological data for middle latitude in evaluation of the integrals leads to the approximate values $K_5=0.3m$ (mb^{-1}) and $K_s=0.7m$ (mb^{-1}). Subtraction of (22) from (27), with the definition (19), then gives

$$\frac{\partial h_d}{\partial t}=-\mathbf{V}_*\cdot\nabla h_d+(K_6+K_4)\omega_m+K_5\omega_0-\mathbf{V}_5\cdot\nabla P'. \tag{28}$$

We can now eliminate ω_m between (28) and (27) to obtain

$$\frac{\partial h_d}{\partial t}=-\mathbf{V}_*\cdot\nabla h_d+\left(1+\frac{K_4}{K_6}\right)\frac{Dh_5}{Dt}$$
$$-\left(\frac{K_5}{\sigma_m K_6}\mathbf{V}_0+\mathbf{V}_5\right)\cdot\nabla P', \tag{29}$$

where

$$\frac{Dh_5}{Dt}\equiv\left(\frac{\partial}{\partial t}+\mathbf{V}_*\cdot\nabla\right)h_5.$$

This latter quantity is to be predicted separately. The ratio $K_4/K_6\approx1$, while $K_5/\sigma_m K_6\approx0.7$. Then, if we define

$$P\equiv1.7P'-800m\approx800\left(\frac{\pi}{1000\text{ mb}}-1\right)m$$

Eq. (29) can be written

$$\frac{\partial h_d}{\partial t}=-\mathbf{V}_*\cdot\nabla h_d+2\frac{Dh_5}{Dt}-(0.41\mathbf{V}_0+0.59\mathbf{V}_5)\cdot\nabla P. \tag{30}$$

For procedural convenience we shall replace the advecting wind in the last term on the right side of (30) by $\mathbf{V}_*$. This term is a crude representation of the orographic effect. Since P is independent of time, the prediction Eq. (30) then becomes

$$\frac{D}{Dt}(h_d+P-2h_5)=0 \tag{31}$$

next we recall from (19) and (20) that

$$h_d-h_{du}=h_{su}-h_s\equiv A(\pi),$$

whence it follows that

$$\frac{D}{Dt}[h_d+P-A-2h_5]=0. \tag{32}$$

In (32) h_d is understood to be the value adjusted for station elevation. This equation asserts that changes in the saturation deficit, following the effective moisture steering flow over smooth terrain, arise from the vertical motions implied by the thickness changes. Thus decreasing thickness implies ascent, which lowers the saturation deficit and tends toward the production of clouds and precipitation, while increasing thickness indicates drying and dissipation of cloud. Over sloping terrain an additional effect enters from variations of the difference $P-A$, illustrated in Table 4. An additional indirect effect will occur since the orographically-induced vertical motions will produce thickness changes which will operate as indicated above. The total effect is in the expected sense. For example, orographic descent would be associated with decreasing values of $P-A$, very likely with increasing thickness and thus with substantial increases of saturation deficit.

TABLE 4. Direct orographic effect, P−A.

π (mb)	1000	950	900	850	800	750	700
$P-A$ (dm)	0	4	8	12	16	21	28

In arriving at Eq. (32) we have made several assumptions and approximations. Therefore, one might question whether the final result is more than remotely related to the theory in Section 3. In defense, we can point out that the effect of horizontal advection remains reasonably intact. The largest errors here will probably stem from determination of $\mathbf{V}_*$ from a constant pressure surface in the vicinity of mountains. The effects of vertical motion (expressed through Dh_5/Dt) are probably large enough to account for the observed statistical relationship between this quantity and cloudiness and precipitation. The simulation of the effects of orography is somewhat dubious and could probably be improved by experimentation. The question of conservation of total virtual precipitable water in the atmosphere cannot be easily examined with Eq. (32). From (32) it is clear that the average value of $(h_d+P-A-2h_5)$ is conserved if $\mathbf{V}_*$ is a nondivergent wind. The relationship of conservation of this quantity to conservation of average W' however, is not clear.

Finally, the model in its present form affords no vertical resolution in the moisture forecast. This defect could be remedied, provided that initial moisture data are adequate, and provided that circulation prognoses have sufficient resolution, by deriving equations similar to (32) for each of a number of arbitrary layers. Vertical moisture transports between layers would be the only complicating factor.

Therefore, since the proof of this pudding must be in the eating, we shall next describe operational problems, present some graphical forecast techniques for integrating Eq. (32), and illustrate with a sample of predictions made at NMC.

6. Forecast interpretation

Certain explanations concerning forecast interpretation are necessary before summarizing the routine detail in applying two forecast equations.

Interpretation of the forecast saturation deficit in terms of separation of clear and cloudy areas is made in approximate conformity with Sanders' statistical evaluation of column relative humidities associated with 50% probability of overcast cloudiness. Cloudy is defined as "overcast" or "overcast with breaks," and is forecast for the area between the zero and 60-gpm saturation deficit isopleths. The 60-gpm saturation deficit isopleth represents approximately 55% column saturation—actually the range being 52% relative humidity with a 4680-gpm thickness to 59% with a 5760-gpm thickness. Since the 70% saturation thickness was selected as the pivotal thickness, a zero saturation deficit indicates 70% column relative humidity and precipitation is forecast within the area bounded by the zero saturation deficit isopleth. Precipitation is verified when precipitation is observed at, or within the hour previous to forecast verification time.

The area within the prognostic zero saturation deficit isopleths will assume negative values which have accumulated during the forecast period, and which may serve as a basis for a satisfactory guide to precipitation volume that would have occurred. The forecast negative saturation deficit isopleths may be evaluated in terms of precipitation depth by use of Table 5. In the example discussed later, the time interval is 24 hours. Accumulation of negative saturation deficits takes place along the 24-hr trajectories so that their location at the end of the forecast period will not give a realistic areal distribution of precipitation depth. Similarly, the end-of-the-period negative deficit does not always represent the total negative deficit produced during the forecast period. This is because downward motion along the latter portion of a trajectory may reduce the negative deficit which had developed earlier.

TABLE 5. Thickness (h) and precipitation depth (D) per 60 gpm of negative saturation deficit ($-h_d$). [Precipitation amount (D) is the net slope of the precipitable water content curve over a 60-gpm interval (30 gpm below to 30 gpm above the designated thickness value) adjusted to obtain conveniently usable values.]

h gpm	D inches	h gpm	D inches
4740	0.01	5340	0.10
4800	0.02	5400	0.12
4860	0.02	5460	0.14
4920	0.03	5520	0.16
4980	0.03	5580	0.18
5040	0.04	5640	0.20
5100	0.04	5700	0.22
5160	0.05	5760	0.25
5220	0.06	5820	0.30
5280	0.08	5880	0.35

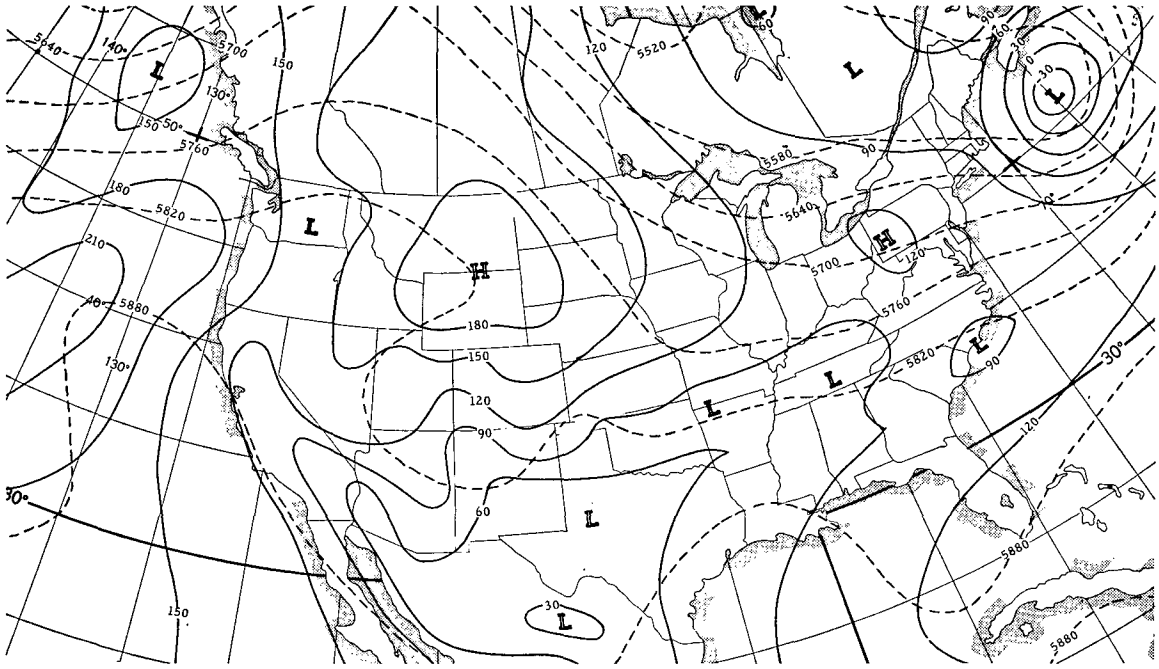

FIG. 2. 1000-mb analysis (solid lines) and 500-mb analysis (dashed lines) for 1200 GCT, 16 June 1963.

In addition to these procedurally caused underestimates of precipitation volume, neglect of the latent heat of condensation's actual contribution to vertical motion further amplifies underestimation of volume. Numerical computation, which will allow both the removal of precipitation in the negative deficit areas and an estimate of latent heat effects at short time intervals should yield more realistic areal distributions of precipitation and will tend to minimize volume errors.

7. Summary of graphical procedures

Eq. (32) integrated in time can be written

$$[h_d+(P-A)-2h_5]^{fd}=[h_d+(P-A)-2h_5]^{iu}, \quad (33)$$

where the superscript *iu* refers to the *initial* value at the *upstream* end of a trajectory representing a displacement over the forecast time step in the $\mathbf{V}_*$-flow field, and where *fd* refers to the *forecast* value at the *downstream* end of this trajectory. Solving for the forecast saturation deficit we may write.

$$h_d{}^{fd}=h_d{}^{iu}-2(h_5{}^{iu}-h_5{}^{fd})+(P-A)^{iu}-(P-A)^{id} \quad (34)$$

since we are neglecting $\partial\pi/\partial t$ so that $(P-A)^{fd}=(P-A)^{id}$. Alternatively

$$h_d{}^{fd}=2h_5{}^{fd}-(h_5+h_s)^{iu}+(P-A)^{iu}-(P-A)^{id}. \quad (35)$$

Use of (34) and (35) leads to Procedures 1 and 2, respectively, which will now be described in some detail. In either case $\mathbf{V}_*$ is taken to be the vector sum of two-thirds of the 1000-mb wind plus one-third of the 500-mb wind. For the utmost simplicity and ease in graphical manipulation, variations of $(P-A)$ are neglected.

SUMMARY OF HAND OPERATED PROCEDURES WITH REFERENCE TO ILLUSTRATED EXAMPLE SHOWN IN FIGS. 2–12.

Procedure I—Eq. (34)

1. Transporting wind field for first 12 hours.
   a) Obtain 500-mb analysis at 60-gpm contour intervals (see Fig. 2).
   b) Obtain 1000-mb analysis at 30-gpm contour intervals (see Fig. 2).
   Double contour values before graphical addition in the next step.
   c) Graphically add 500- and 1000-mb analyses and divide by 3 to obtain transporting wind field at 20-gpm intervals.

2. Moisture field.
   a) Convert observed precipitable water into unadjusted saturation thickness using Table 2.
   b) Correct unadjusted stturation thickness using Table 3, then analyze saturation thickness at 60-gpm intervals (see Fig. 3).
   c) Obtain 1000- to 500-mb thickness analysis at 60-gpm contour intervals (see Fig. 4).
   d) Graphically subtract saturation thickness analysis from 1000- to 500-mb thickness analysis. This is the saturation deficit chart (see Fig. 5).

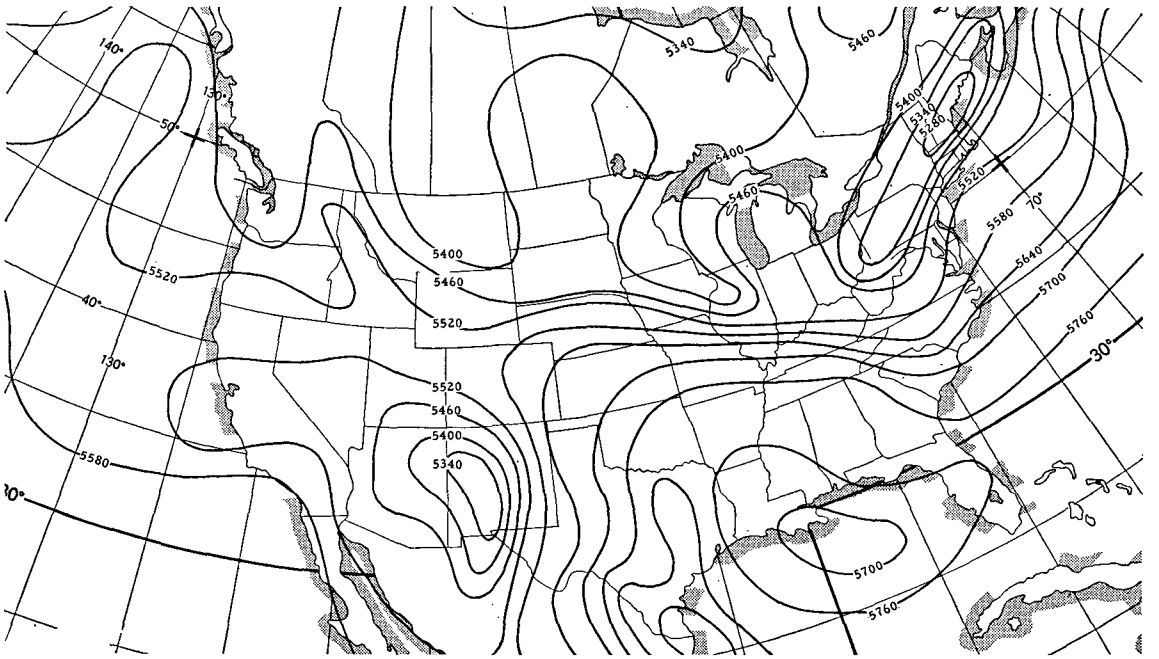

FIG. 3. Saturation thickness analysis for 1200 GCT, 16 June 1963.

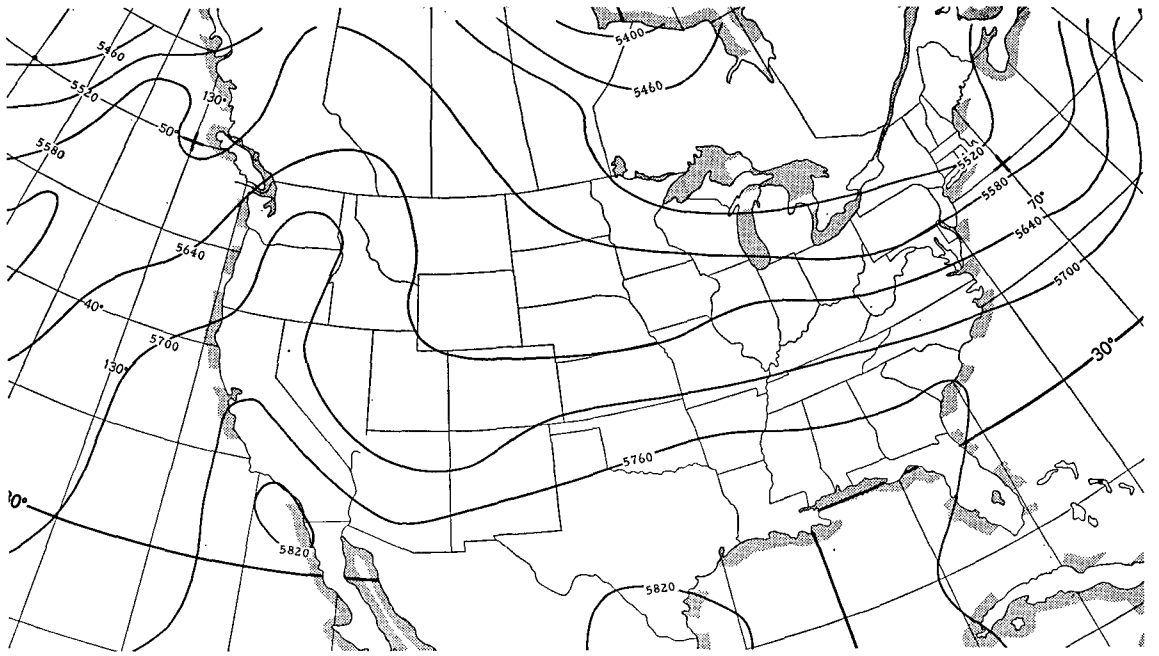

FIG. 4. 1000-500-mb thickness analysis for 1200 GCT, 16 June 1963.

3. First 12-hr transportation of saturation deficit and observed thickness.
   a) Transport saturation deficit along with 100 per cent of geostrophic wind obtained from 1-c.
   b) Similarly advect 1000- to 500-mb thickness.
4. Transporting wind field for second 12 hours. Repeat 1-a thru c using 24-hr 500- and 1000-mb prognostic charts (Fig. 6) in obtaining advective field.
5. Second 12-hr transportation of saturation deficit and thickness.

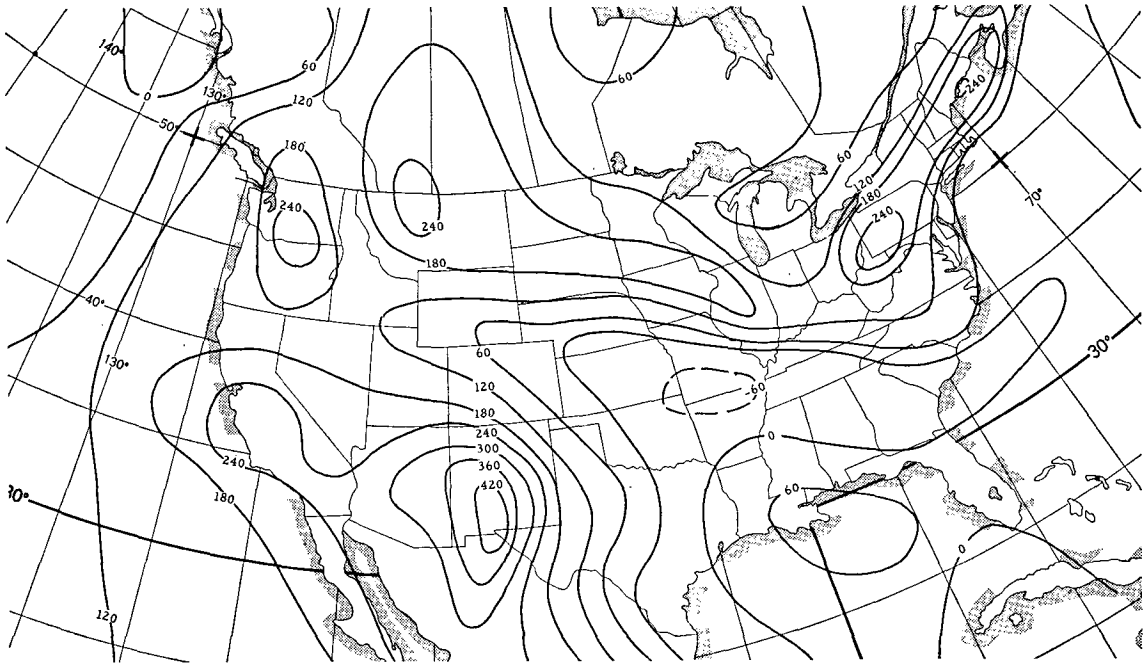

FIG. 5. Derived saturation deficit for 1200 GCT, 16 June 1963.

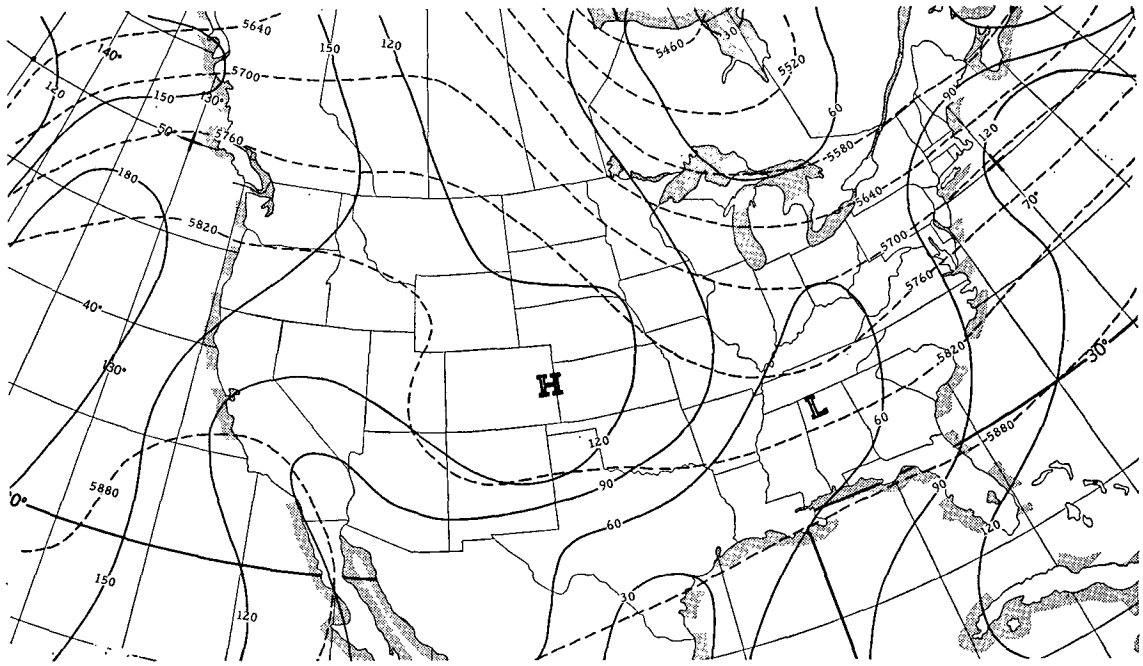

FIG. 6. 24-hr 1000-mb prognosis (solid lines) and 500-mb prognosis (dashed lines) verifying at 1200 GCT, 17 June 1963.

a) Transport saturation deficit noting that measured advection must be applied upstream (see Fig. 7).
b) Similarly advect 1000-mb to 500-mb thickness (see Fig. 8).

6. Derivation and application of vertical motion field.

a) Need 24-hr 1000- to 500-mb thickness forecast obtained through subtraction of 24-hr 1000-mb prognosis from 500-mb prognosis (see Fig. 9).
b) Subtract 24-hr thickness forecast from 24-hr advected thickness to obtain dynamic thickness change.
c) Multiply difference by 2 to obtain vertical mo-

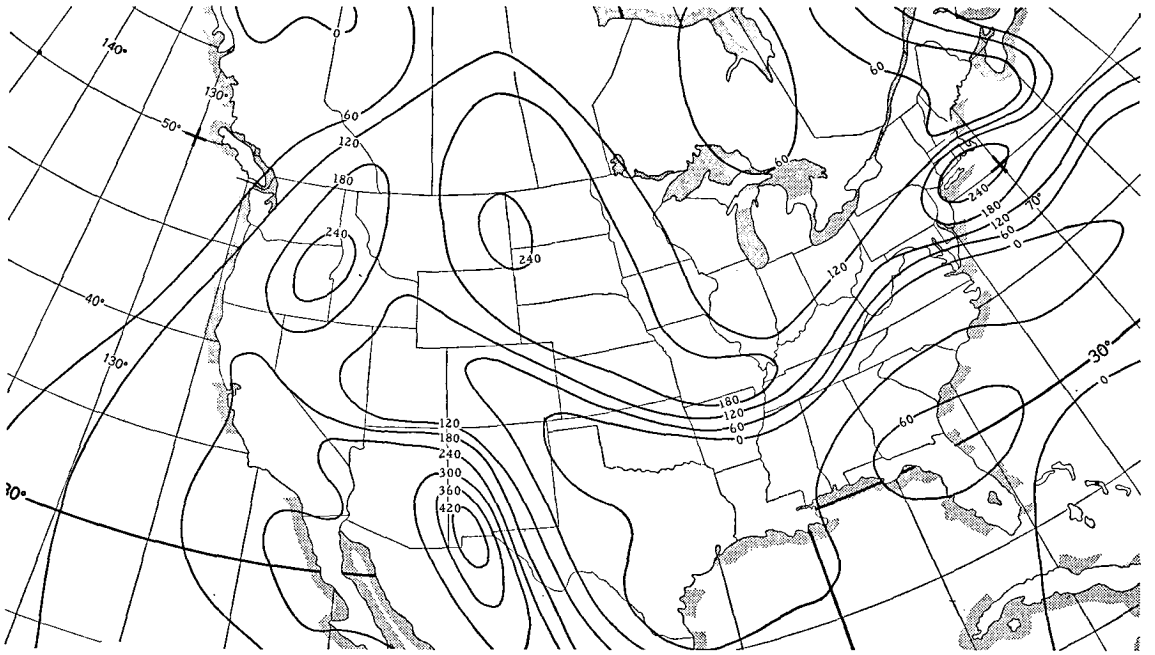

FIG. 7. 24-hr advected saturation deficit for period ending at 1200 GCT, 17 June 1963.

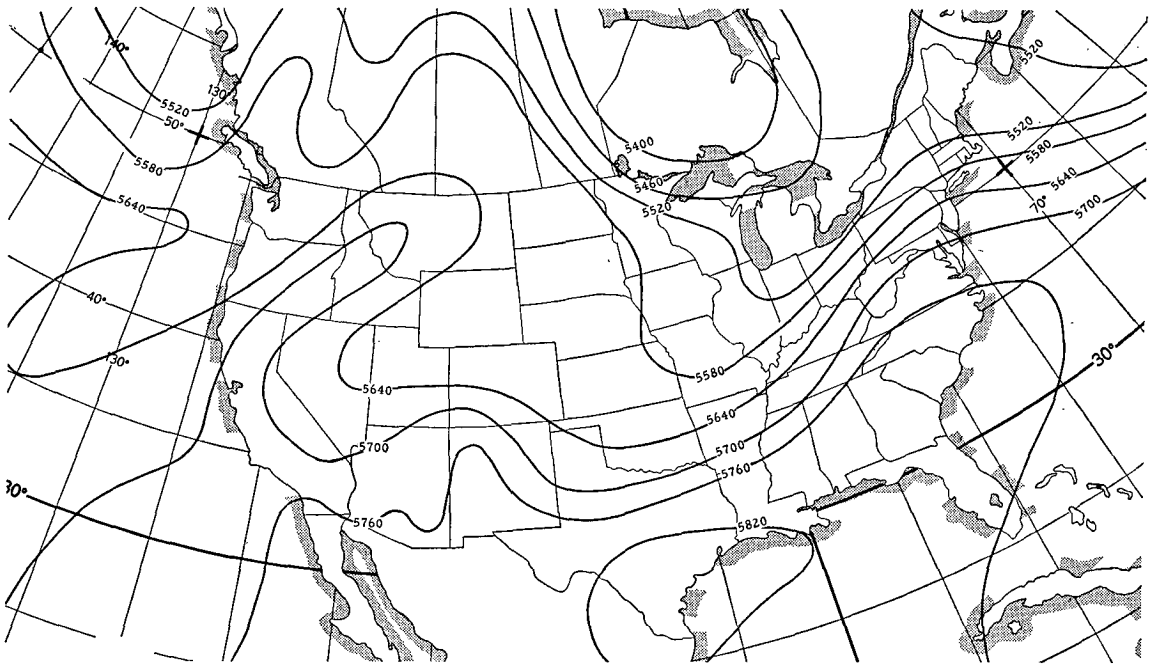

FIG. 8. 24-hr. advected 1000–500-mb thickness for period ending at 1200 GCT, 17 June 1963.

tion in terms of saturation thickness change (see Fig. 10).

d) Add graphically the saturation thickness change to the 24-hr transported saturation deficit to obtain a saturation deficit forecast (see Fig. 11).

7. Forecast (see Fig. 12).

a) Forecast 50 per cent or greater probability of precipitation occurrence for the areas where the saturation deficit ≤ 0.

b) Forecast overcast for areas where the saturation deficit >0 but ≤ 6.

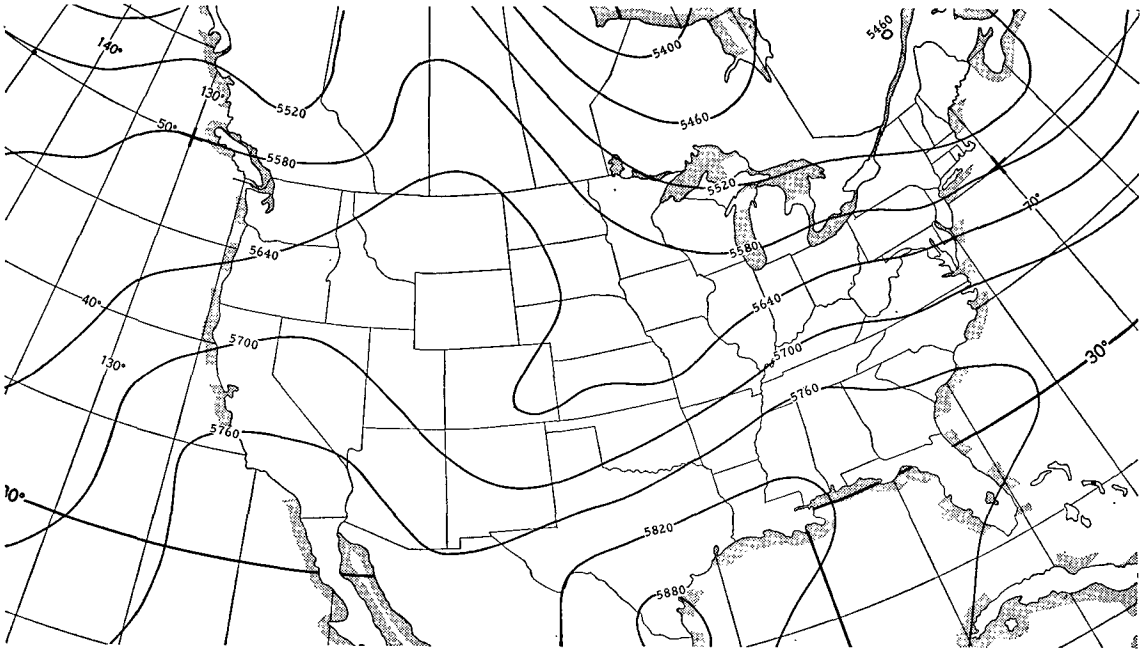

FIG. 9. 24-hr objective forecast of the 1000–500-mb thickness verifying at 1200 GCT, 17 June 1963.

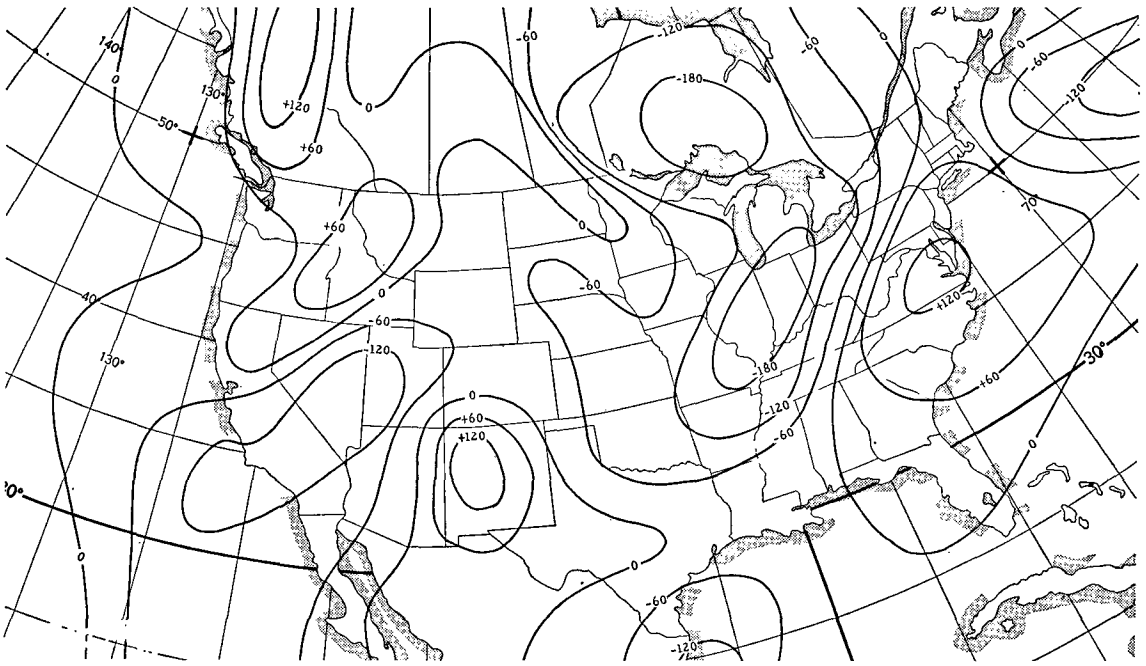

FIG. 10. 24-hr time-integrated vertical motions in terms of saturation thickness change for period 1200 GCT, 16 June 1963 to 1200 GCT, 17 June 1963.

Procedure II—Eq (35)

1. Same as Procedure I,1.
2. Moisture field.

   a, b, c) Same as Procedure I-2a through 2c.

   d) Add graphically the saturation thickness and the 1000–500-mb thickness.

3, 4, 5. Same as Procedure I-3, 4, and 5 except that the combination thicknesses produced in 2d are transported.

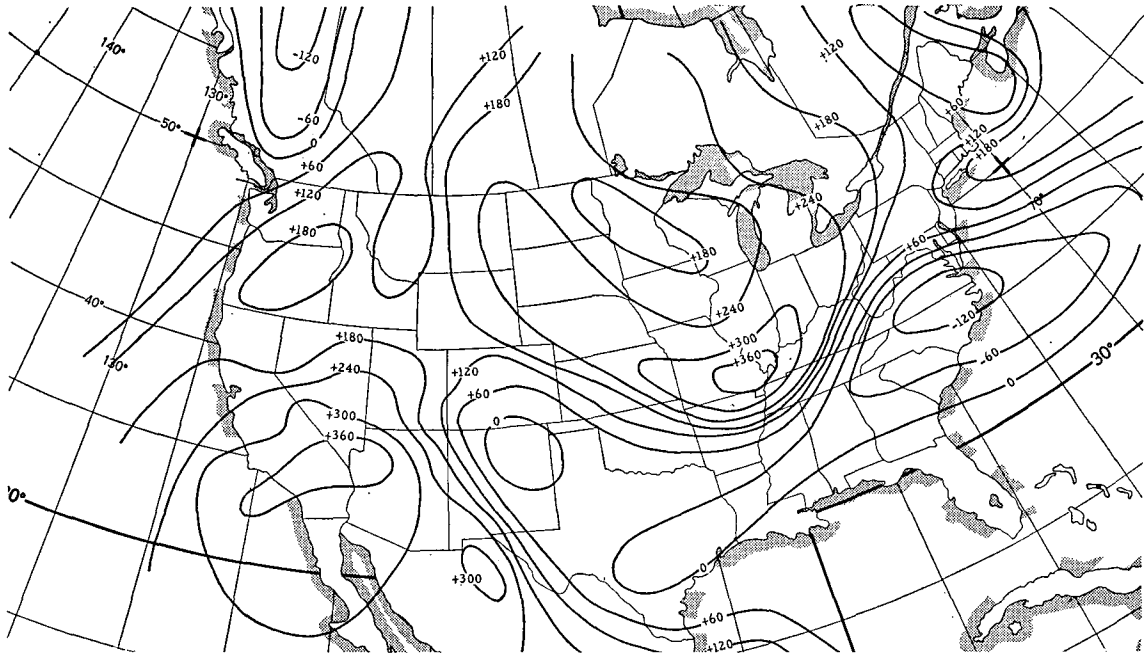

FIG. 11. 24-hr forecast of the saturation deficit verifying at 1200 GCT, 17 June 1963.

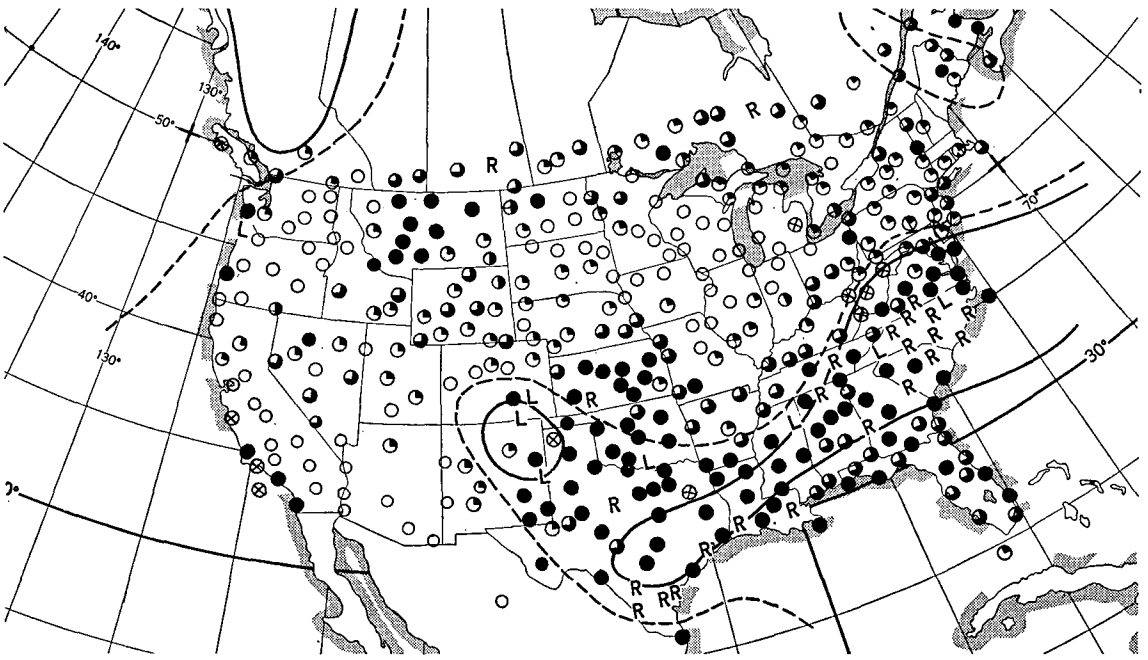

FIG. 12. 24-hr forecast precipitation (solid lines) and overcast (dashed lines) superimposed on observed cloud and precipitation chart for 1200 GCT, 17 June 1963. The observed sky-cover was deleted when precipitation was reported.

6. Extraction of forecast moisture field.
   a) Obtain 24-hr forecast 1000–500-mb thickness and multiply by 2.
   b) Subtract 24-hr advected combined thicknesses from doubled forecast thickness to obtain saturation deficit.
7. Forecast clouds and precipitation as in Procedure I.

8. Summary

Improvement in cloud and precipitation forecasting has been lagging improvement made in some of the other phases of meteorological prediction. This lag has occurred despite the increased guidance provided by numerical circulation prognoses.

Proposed objective cloud and precipitation forecast

schemes applicable to large areas have been unable to compete with subjective methods. The use of moisture data for only significant levels and use of vertical motions insufficient in magnitude and often times inconsistent with surface circulations have been the two main difficulties. The forecast technique presented here largely overcomes these two problems. Vertically-integrated moisture is operated upon by time-integrated vertical motions which are completely consistent with the 1000-mb and 500-mb horizontal motion fields. Two operational procedures are outlined in detail and example charts given for the first of these.

This system also can make quantitative predictions of precipitation through treatment of negative saturation deficits as precipitation amounts. Only a moderately reasonable areal-depth distribution of precipitation is obtained in hand operation, since extraction of excess water vapor is not practical until the end of the period. Also, with the long time steps in hand operation, the forecast precipitation volume is necessarily underestimated, because periods of downward vertical motion prior to the end of the forecast period will reduce the excess water vapor which accumulated earlier in a general upward motion field. Due to the feasibility of short time-steps, numerical operation will relieve both of these difficulties.

The Development Division of NMC has completed the programming of this simple model and routine operational IBM 7094 output for 12-hr periods out to 48 hours after initial data time was begun on 15 September 1964. Thus far, the cloud and weather forecasts have been most encouraging. The quantitative precipitation forecasts have been moderately useful as numerical guidance in preparation of this type forecast. Latent heat is included in the computer quantitative precipitation product.

Acknowledgments. We wish to thank Mrs. Jane Violett, Mr. Joseph L. Mullaney, Mr. Paul Goree, and Mr. Vernon Bohl of the Analysis and Forecast Division of NMC for preparation of figures and helpful comments and suggestions. Also, we wish to express our gratefulness to Professor Norman A. Phillips of the Massachusetts Institute of Technology for time spent in fruitful discussions with Professor Sanders.

REFERENCES

Collins, G. O., and P. M. Kuhn, 1954: A generalized study of precipitation forecasting, Part 3. *Mon. Wea. Rev.*, **82**, 173–182.

Estoque, M. A., 1956: An approach to quantitative precipitation forecasting. *J. Meteor.*, **13**, 50-54.

George, J. J., *et al.*, 1960: Pre-trough winter precipitation forecasting. *Weather Forecasting for Aeronautics*, New York, Academic Press, pp. 373–406.

Kuhn, P. M., 1953: A generalized study of precipitation forecasting, Part 2. *Mon. Wea. Rev.*, **81**, 222–232.

Penner, C. M., 1963: An operational method for the determination of vertical velocities. *J. Appl. Meteor.*, **2**, 235–241.

Phillips, N. A., 1957: A coordinate system having some special advantages for numercial forecasting. *J. Meteor.*, **14**, 184–185.

Reed, R. J., 1963: Experiments in 1000-mb prognosis. Washington, D. C., U. S. Weather Bureau, National Meteorological Center Technical Memoradum No. 26, 1–31.

Reitan, C. H., 1963: Surface dew point and water vapor aloft. *J. Appl. Meteor.*, **2**, 776–779.

Sanders, F., 1958: Cloudiness and precipitation in relation to large scale vertical motion and moisture. Boston, Mass., Massachusetts Institute of Technology, Dept. of Meteorology, Scientific Report No. 4,1–30, Contract No. AF19(604)-1305. [Available from U. S. Weather Bureau, Washington, D.C.]

——, 1963: A prediction model for integrated water vapor, cloudiness and precipitation, in Final Report Contract No. AF19(604)-8373, Dept. of Meteorology, M.I.T. [Available from Dept. of Meteorology, M.I.T., Cambridge, Mass.]

Showalter, A. K., 1954: Precipitable water template. *Bull. Amer. Meteor. Soc.*, **35**, 129–131.

Smagorinsky, J., and G. O. Collins, 1955: On the numerical prediction of precipitation. *Mon. Wea. Rev.*, **83**, 53–57.

Smebye, S. J., 1958: Computation of precipitation from large scale motion. *J. Meteor.*, **15**, 547–560.

Solot, S. B., 1939: Computation of depth of precipitable water in a column of air. *Mon. Wea. Rev.*, **67**, 100–103.

Spar, J., 1963: A suggested technique for quantitative precipitation forecasting. *Mon. Wea. Rev.*, **81**, 217–221.

Staff Members, Tokyo University, 1955: The quantitative forecast of precipitation with the numerical method. *J. Meteor. Soc. Japan*, **33**, 204–216.

Sutcliffe, R. C., and A. G. Forsdyke, 1950: The theory and use of thickness patterns in forecasting. *Quart. J. R. Meteor. Soc.*, **76**, 189–217.

Swayne, W. W., 1956: Quantitative analysis and forecasting of winter rainfall patterns. *Mon. Wea. Rev.*, **84**, 53–65.

Thompson, J. C., and G. O. Collins, 1953: A generalized study of precipitation forecasting, Part 1. *Mon. Wea. Rev.*, **81**, 91–100.

Vederman, J., 1961: Forecasting precipitation with the aid of a high-speed electronic computer. *Mon. Wea. Rev.*, **89**, 243–250.